Appl Microbiol Biotechnol (2003) 62:244–255
DOI 10.1007/s00253-003-1257-z

ORIGINAL PAPER

Md. M. Kabir · K. Shimizu

Fermentation characteristics and protein expression patterns in a recombinant *Escherichia coli* mutant lacking phosphoglucose isomerase for poly(3-hydroxybutyrate) production

Received: 30 October 2002 / Revised: 21 December 2002 / Accepted: 3 January 2003 / Published online: 20 March 2003

Abstract For the efficient production of poly(3-hydroxybutyrate) (PHB) using recombinant *Escherichia coli*, it is of primal importance to overproduce NADPH, which is necessary for the PHB synthetic pathway. In order to overproduce NADPH in the pentose phosphate (PP) pathway, a recombinant *E. coli* was constructed in which the phosphoglucose isomerase (*pgi*) gene was knocked out to force the carbon flow into the PP pathway. The fermentation characteristics of the recombinant *E. coli* mutant lacking *pgi* were then investigated to determine the effect of overproduction of NADPH on efficient PHB production. It was found that, compared with the parent strain (*E. coli* JM109), growth of the *E. coli* mutant lacking *pgi* (*E. coli* DF11) is repressed due to NADPH overproduction in the PP pathway. Furthermore, repressed cell growth can be recovered to some extent by introducing a NADPH-consuming pathway, such as the PHB synthetic pathway. Efficient PHB production using such recombinant *E. coli* (DF11/pAeKG1) could be attained by appropriately controlling the glucose concentration in the fermentor. Total gene expression was investigated at the protein level by two-dimensional electrophoresis. Out of 22 differentially expressed proteins, 12 were identified with the aid of MALDI-TOF mass spectrometry. Variations in the accumulation of PHB in the recombinant *pgi* mutant carrying *phb* (*E. coli* DF11/pAeKG1) corresponded to the expression of proteins encoded by *rpsA, znuA, fabD, potD, fkpA, gapA, ynaF* and *ibpA*. The unfavorable conditions generated by PHB accumulation in the *pgi* mutant carrying *phb* resulted in the highest expression of 30S ribosomal protein S1, which ultimately caused a further increase in soluble protein synthesis.

M. M. Kabir · K. Shimizu
Department of Biochemical Engineering and Science,
Kyushu Institute of Technology,
820–8502 Iizuka, Fukuoka, Japan

K. Shimizu (✉)
Institute for Advanced Biosciences,
Keio University,
997–0017 Tsuruoka, Yamagata, Japan
e-mail: shimi@bse.kyutech.ac.jp
Tel.: +81-0948-297817
Fax: +81-0948-297801

Introduction

Poly-3-hydroxybutyrate (PHB) is a homopolymer of 3-hydroxybutyrate and is the most widespread and best-characterized member of the poly-β-hydroxyalkanoates (PHAs). The genes involved in PHB biosynthesis in *Ralstonia eutropha* were cloned in *Escherichia coli*, sequenced, and characterized in detail (Peoples and Sinskey 1989; Schubert et al. 1988; Slater et al. 1988). Since then, much effort has been devoted to enhancing expression of the *phb* operon (Kalousek and Lubitz 1995; Kidwell et al. 1995; Sim et al. 1997; Shi et al. 2001), increasing plasmid stability (Lee et al. 1994a), and decreasing filamentation (Lee 1994). Less attention has been paid to modification of *E. coli* metabolism. For efficient PHB production using recombinant *E. coli*, the major limiting factors are a shortage of NADPH necessary for the reaction catalyzed by acetoacetyl-CoA reductase and acetyl-CoA. Since NADPH is mainly formed in the pentose phosphate (PP) pathway in *E. coli*, we constructed a phosphoglucose isomerase (*pgi*) knockout *E. coli* for PHB production (Shi et al. 1999). Inactivation of *pgi* in *E. coli* shifts glucose catabolism to the the hexose monophosphate shunt (HMP) (Fig. 1). As a consequence, metabolic redirection in a *pgi* mutant provides more NADPH, and thus may enhance PHB synthesis in recombinant *E. coli* carrying *phb*.

To study the altered overall cellular physiology in the *pgi* knockout recombinant *E. coli*, it is important to regard the complex biological systems in their entirety, rather than as a multitude of individual components. Proteomics is a newly emerging research field that allows such complex biological systems to be investigated as a whole because it facilitates simultaneous analysis of total gene expression at the protein level (Blackstock and Weir

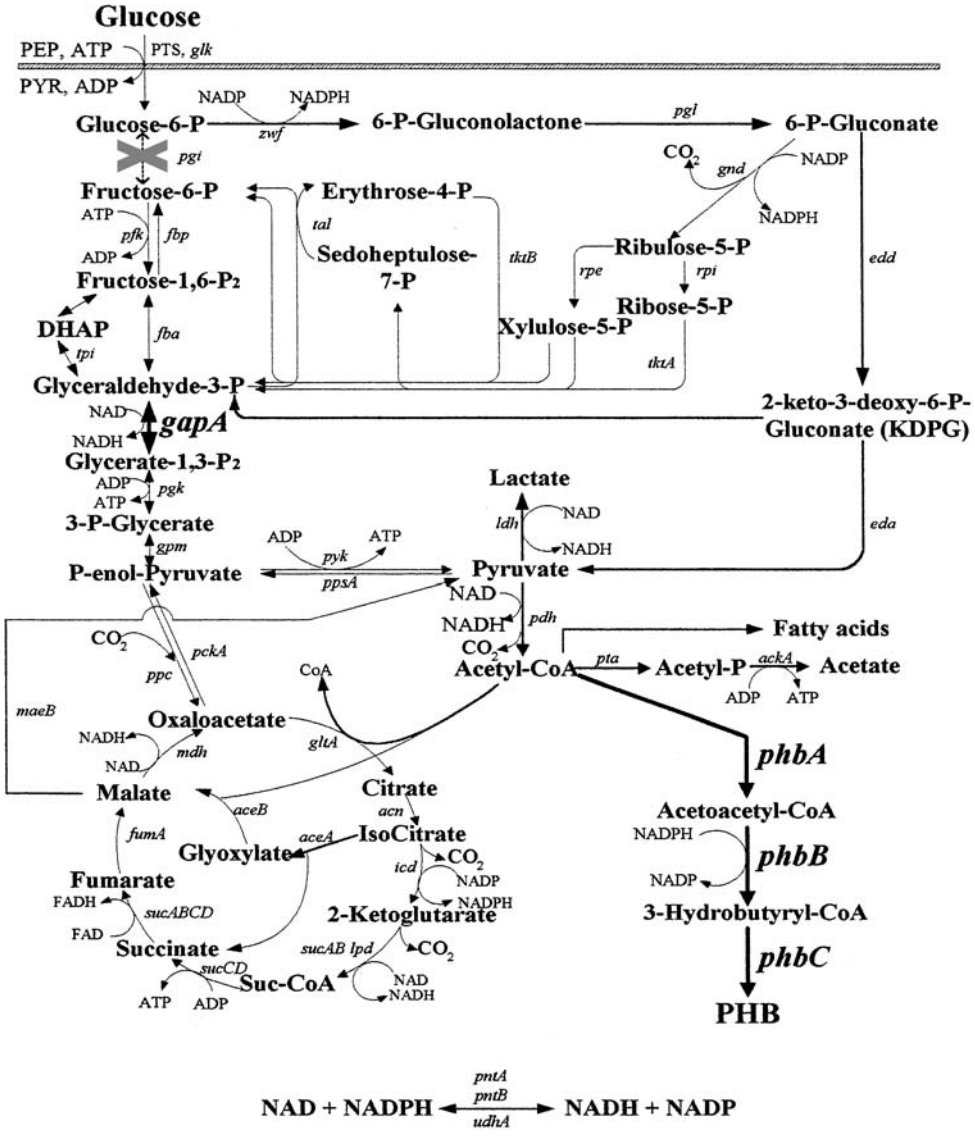

Fig. 1 Central metabolic reaction network of the recombinant *Escherichia coli* involved in metabolic engineering for PHB production. The protein encoded by *gapA* and the reaction step that it catalyzes are shown in *bold*. The reaction pathways concerning with the synthesis of PHB along with the enzymes involved are also shown in *bold*. *DHAP* Dihydroxyacetone phosphate

1999; Hochstrasser 1998; Persidis 1998). Proteome analysis by two-dimensional gel electrophoresis has been proposed as a powerful tool for developing functional applications of genomics (Blackstock and Weir 1999; Hochstrasser 1998; Hochstrasser et al. 1998; Persidis 1998; O'Farrell 1975). Of equal importance is mass spectrometry supported by the matrix-assisted safe ionization of peptide fragments and delayed extraction of the peptide fragments for the purpose of enhancing resolution power (Pappin et al. 1993; Patterson 2000). These extended capabilities of mass spectrometry, along with the ever-increasing amount of protein sequence data in various databases, make protein identification and characterization feasible.

In the present study, we investigated the fermentation characteristics of the *pgi* knockout *E. coli* carrying *phb* for the biosynthesis of PHB. Protein expression patterns were also studied using 2D gel electrophoresis and MALDI-TOF mass spectrometry. In addition, we compared protein expression with gene expression using RT-PCR.

Materials and methods

Bacterial strains, plasmids, and growth conditions

The strains used in the present study were *E. coli* DF11 (*rpsL176* [*strR*] *metA28 pgi-2 his-84*) and *E. coli* DF11/pAeKG1 having a plasmid that contains the *Ralstonia eutropha* PHB biosynthesis genes (Shi et al. 1999). These genes are constitutively expressed in *E. coli*. As a control, *E. coli* JM109 (*recA1 supE44 hsdR17 endA1 gyrA96 thi relA1* Δ[*lac proAB*] *ka*) was also cultivated. Luria-Bertani (LB) medium containing 20 g glucose/l as the sole carbon source was used for cell growth. The inoculum was prepared by transferring cells from a glycerol stock (0.1 ml) to a 50-ml L-shaped test tube containing 10 ml of LB medium. The culture was incubated overnight, and 1 ml of the broth was then transferred into a 500-ml T-shaped flask containing 100 ml of LB medium. Ampicillin (50 μg/ml) was added to maintain the plasmid. Batch fermentation was carried out in a 2-l jar fermentor (M-100,

Rikakikai, Tokyo) containing 1 l of LB medium sterilized for 20 min at 121 °C. Fed-batch fermentation was carried out in a 5-l jar fermentor (MDL 500–5L, Marubishi, Japan) equipped with an on-line glucose sensor (BF-400, Able); the working medium was 3 l. The culture temperature was maintained at 37 °C and the pH was maintained at 7 by adding 4 N NaOH.

Analytical procedures

Cell concentration was determined by measuring the optical density (OD) of the culture broth with a spectrophotometer (Ubet-30, Jasco Co., Tokyo) at 600 nm. The OD value was then converted to g DCW (dry cell weight)/l using the relationship between OD values and DCW obtained previously. The amount of PHB was measured by gas chromatography (GC-8APF/C-R6A, Shimadzu, Kyoto) as described by Braunegg et al. (1978). Acetic acid, lactic acid, and glucose concentrations were measured using enzyme kits (Wako, Osaka, Japan). Intracellular NADPH concentration was measured according to the method of Bergmeyer (1989).

Protein and enzyme assays

Folin and Ciocalteu's phenol reagent was used to determine protein concentration using a method was similar to that described by Lowery et al. (1951). A standard curve was constructed for each experiment using crystalline bovine serum albumin (Sigma, USA). For enzyme assays, aliquots were removed at the indicated time intervals, centrifuged and frozen at −20 °C. The samples were then thawed on ice, washed with 0.1 M Tris-HCl (pH 7.5) buffer, and resuspended in a 10% volume of the same buffer. Cells were disrupted by sonication and clear supernatant was collected by centrifuge at 4 °C. Phosphoglucose isomerase and malic enzyme activities were assayed according to the method described by Salas et al. (1965) and Van der Werf et al. (1997), respectively.

Sample preparation for 2 DE

Cells were grown aerobically in LB medium and harvested. The culture medium was centrifuged for 30 min at 4,000 rpm at 4 °C, and the pellet was washed four times for 10 min at 3,000 rpm in low-salt washing sample buffer (Kabir and Shimizu 2001). The washed pellet was then resuspended in a lysis solution containing 8 M urea, 2% Triton X-100, 40 mM Tris (base) and 2 mM PMSF (protease inhibitor). This solution was sonicated at 10% maximum output on ice for 1 min (four cycles of sonication, each for 15 s) in an ultrasonic disrupter (UD-201, Tomy, Tokyo, Japan). After sonication, the solution was centrifuged again at 12,000 rpm for 15 min at 4 °C to sediment the cell debris and insoluble proteins, and stored in 50-μl aliquots at −20 °C. Fifty μg of *E. coli* proteins, which corresponds to the appropriate volume of frozen samples, were resuspended in 20 μl of a solution containing 8 M urea, 2% Triton X-100, 35 mM Tris and 65 mM dithiothreitol (DTT). This sample mixture was loaded onto a rehydrated IPG (immobilized pH gradient) strip in a DryStrip aligner via a sample cup after IPG strip rehydration.

Isoelectric focusing and 2D SDS-PAGE

Isoelectric focusing (IEF) was carried out on 18-cm, pH 3–10 nonlinear IPG strips (Amersham Pharmacia Biotech, Sweden). The IPG strips, which have an immobilized pH gradient to improve reproducibility, were rehydrated overnight at room temperature in the Immobiline DryStrip Reswelling tray (Amersham Pharmacia Biotech) with the rehydration solution prepared according to the manufacturer's protocol. After rehydration, IEF was run using the following conditions: (1) 500 V, 5 Vh; (2) 3,500 V, 5250 Vh; (3) 3,500 V, 22,166 Vh. Voltage increases were made on a "gradient" basis. After IEF, gels were equilibrated in two steps by adding 1% DTT and 2.5% iodoacetamide with SDS-equilibration buffer stock solution according to the manufacturer's protocol. Two dimensional SDS-PAGE) was done using the Multiphor II flatbed system and ExcelGel XL SDS 12–14% T (Amersham Pharmacia Biotech).

Silver staining and image analysis

Proteins were stained using an ammoniacal silver-staining method, and all steps were carried out using the Hoefer Automated Gel Stainer (Amersham Pharmacia Biotech). Silver-stained gels were scanned as described previously (Kabir and Shimizu 2001). The gels were analyzed by visual inspection and the computer-assisted gel analysis software Image Master 2D Elite (Amersham Pharmacia Biotech) to automate the process of detecting spots within the image. To check the reproducibility and to estimate standard deviations, protein samples taken from duplicate cultures were analyzed in duplicate 2D gels. The intensities of the spots in the different gels were normalized using the "normalize" function in the image analysis software. In our study, the normalized volume for a spot was calculated by dividing its volume by the total volume of the spots detected on the image. Since this tends to produce extremely small values, the result was multiplied by a constant value, 100, which gives the spot percentage volume.

Reduction and alkylation of gel spots

Differentially expressed protein spots were excised from the gel and in-gel digested with trypsin according to a published procedure (Rosenfeld et al. 1992) using the modification of Shevchenko et al. (1996). A control piece of gel was cut from a blank region of the gel and processed in parallel with the sample. In contrast to the protocol described for Coomassie-stained gels, all prewashing steps were omitted. The gel pieces were excised, shrunk by dehydration in acetonitrile, which was then removed, and dried in a freeze dryer. A volume of 10 mM DTT in 100 mM NH_4HCO3 sufficient to cover the gel pieces was added, and the proteins were reduced for 1 h at 56 °C. After cooling at room temperature, the DTT solution was replaced with the same volume of 55 mM iodoacetamide in 100 mM NH_4HCO3. After a 45-min incubation at room temperature in the dark with occasional vortexing, the gel pieces were washed with 100 μl of 100 mM NH_4HCO3 for 10 min, dehydrated by addition of acetonitrile, swelled by rehydration in 100 mM NH_4HCO3, and shrunk again by addition of the same volume of acetonitrile. The liquid phase was removed, and the gel pieces were completely dried in a freeze dryer. The gel pieces were then swollen in digestion buffer containing 50 mM NH_4HCO3, 5 mM $CaCl_2$, and 20 ng/μl of sequencing grade trypsin (Boehringer Mannheim, Mannheim, Germany) in an ice-cold bath. After 45 min, the supernatant was removed and replaced by the same buffer, but without trypsin, to keep the gel pieces wet during enzymatic cleavage. Trypsin digestion was carried out overnight at 37 °C in a stationary incubator.

Peptide-mass fingerprinting

In-gel digested peptide fragments were extracted from gel pieces by addition of 50 μl of 60% (v/v) acetonitrile and 0.1% (v/v) trifluoroacetic acid (TFA) solution, followed by vortexing for 1 h. After transferring the supernatant solution into a new Eppendorf tube, acetonitrile-TFA solution was added for the final extraction of the remaining peptide fragments at room temperature. After these two supernatant solutions were combined, solute materials including peptide fragments were dried down in a freeze dryer. The samples were passed through a ZipTip coloum (Millipore, Bedford, Mass., USA) in which C_{18} resin is fixed at the end of the tip to eliminate impurities such as salt molecules and gel particles. α-Cyano-4-hydroxycinamic acid, saturated in a solution composed of 50% (v/v) acetonitrile and 0.1% (v/v) TFA, was used as matrix for matrix-assisted laser desorption ionization time-of-flight (MALDI-

TOF) mass spectrometry. This matrix was incorporated with contaminant-free peptide fragments, placed on the sample plate, and crystallized with the peptide sample by air drying. The MALDI-TOF MS system used was the Voyager Biospectrometry system (PerSeptive Biosystems, Framingham, Mass., USA). Laser intensity for the ionization of samples was optimized between 2,500 and 2,700. The accelerating voltage for the flight of ionized particles was 21,000 V, and the delayed extraction time was set at 150 ns. Two standard peaks of 861.25 (*m/z*) and 2,388.67 (*m/z*) were generated from the trypsin autolytic reaction. Other peptide fragment peaks that are usually placed between these two standard peaks were calibrated using the values of these two standard peaks. Due to the unavailability of the ProteinProspector server (http://prospector.ucsf.edu/ucsfhtml 3.4/msfit.htm) at the time of our investigation, the PeptIdent server (http://us.expasy.org/tools/peptident.html) was used for the identification and characterization of protein spots by querying the trypsin-digested peptide fragment data. To maintain the highest certainty of protein identification, mass tolerance was set within ±0.2 Daltons. The reference database used for the identification of target proteins was SWISS-PROT and TrEMBL (http://www.expasy.ch/sprot).

RNA isolation and semi-quantitative RT-PCR

Total RNA was isolated from *E. coli* cells by Qiagen RNeasy Mini Kit (Qiagen, Japan) according to their protocol. The quantity and purity of the RNA were determined by optical density measurements at 260 and 280 nm and by 1% formaldehyde agarose-gel electrophoresis. The following primers were used for RT-PCR reactions and were synthesized at GENSET KK (Kyoto, Japan). *rpsA* primers: forward 5'-GCTCAACTCTTTGAAGAGTC-3', reverse 5'-TCGCCTTTAGCT GCTTTGAA-3'; *greA* primers: forward 5'-ATGCAAGCTATTCCGATGAC-3', reverse 5'-CAGGTATTCCACCTTAATTAC-3'; *gapA* primers: forward 5'-GTAGGTATCAA CGGTTTTGGC-3', reverse 5'-TTTGGAGATGTGAGCGATCA-3'; *ptsG* primers: forward 5'GAATGCATTTGCTAACCTGCA-3', reverse 5'-CGGATGTACTCATCC ATCTCG-3'. RT-PCR reactions were carried out in a TaKaRa PCR Thermal Cycler (TaKaRa TP240, Japan) using Qiagen OneStep RT-PCR Kit. The reaction mixture was incubated for 30 min at 50 °C for reverse transcription followed by 15 min incubation at 95 °C for initial PCR activation. Subsequently, the reaction was subjected to 30 cycles of amplification consisting of a denaturing step (94 °C for 1 min), an annealing step (approximately 5 °C below T_m of primers for 1 min) and an extension step (72 °C for 1 min); final extension was carried out for 10 min at 72 °C. To check for nucleic acid contamination, one negative control, in which template RNA was lacking, was run in every round of RT-PCR. Five microliters of amplified products were run on a 2% agarose gel. Gels were stained with 1 μg ethidium bromide/ml, photographed using a Digital Image Stocker (DS-30, FAS III, Toyobo, Osaka, Japan) under UV light, and analyzed using Gel-Pro Analyzer 3.1 (Toyobo) software. The PCR products obtained for all the genes had the predicted sizes on agarose gel. In order to determine the optimal amount of input RNA, the two-fold-diluted template RNA was amplified in RT-PCR assays under identical reaction conditions to construct a standard curve for each gene product. When the optimal amount of input RNA was determined for each gene product, RT-PCR was carried out under identical reaction conditions to detect differential transcript levels of genes. The gene *dnaA*, which encodes *E. coli* DNA polymerase and is not subjected to variable expression, i.e. abundant expression at relatively constant rates in most cells, was used as an internal control in the RT-PCR determinations.

Results

Batch cultures of recombinant *pgi* knockout *E. coli* DF11/pAeKG1 carrying *phb* were conducted in LB medium containing 20 g glucose/l in which the dissolved oxygen (DO) concentration and pH were maintained at about 3 ppm and 7, respectively, with the aid of computer control. Batch cultures of *pgi* mutant *E. coli* DF11 lacking *phb* and *E. coli* JM109 were also conducted for comparison. Figure 2 shows the batch experimental results for these three strains. Table 1 shows the true cell mass, obtained by subtracting the PHB concentration from the biomass; the soluble protein concentration; and the acetic acid and lactic acid concentrations at the time shown by the arrow in Fig. 2 for proteome analysis. The PHB concentration and PHB content obtained from *E. coli* DF11/pAeKG1 at the time of proteome analysis were 0.63 g/l (see Fig. 2c) and 10.71%, respectively. The enzyme activities of *pgi* at the time of proteome analysis were 0.417±0.01, 0.019±0.02 and 0.024±0.02 U/mg protein for *E. coli* JM109, *E. coli* DF11 and *E. coli* DF11/pAeKG1, respectively. Figure 2a, b shows that

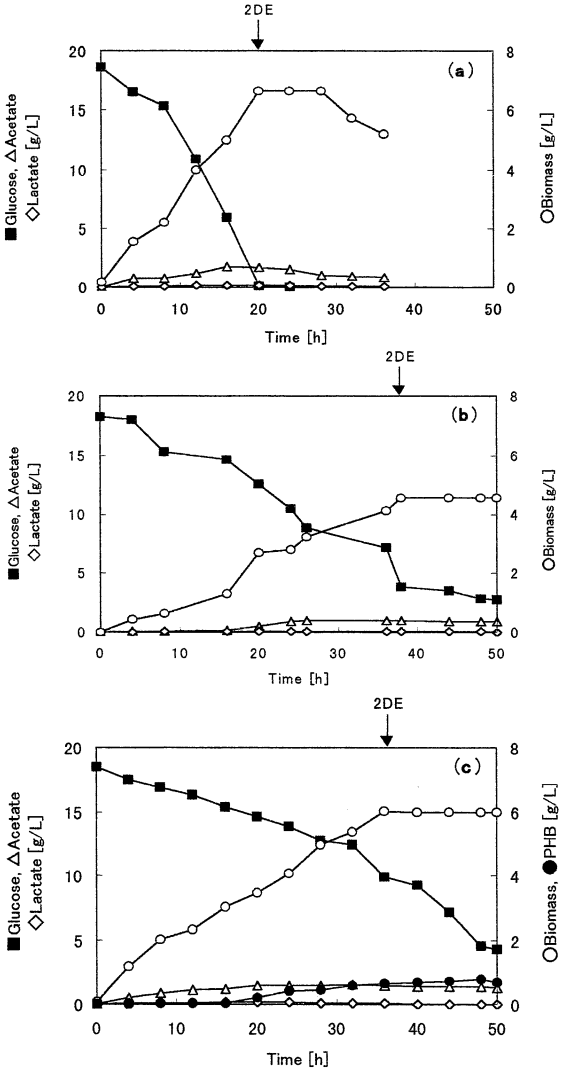

Fig. 2 Results of batch-fermentation of **a** *E. coli* JM109, **b** *E. coli* DF11, and **c** *E. coli* DF11/pAeKG1. *Arrow* Sampling time for proteome analysis

Table 1 Comparison of biomass, extracted soluble protein, acetate and lactate concentrations at the time of harvesting for proteome analysis. *DCW* Dry cell weight

Strain	True cell mass[a] (g DCW/l)	Soluble protein[a] (mg/ml)	Acetate[a] (g/l)	Lactate[a] (g/l)
DF11/pAeKG1	5.38±0.05	2.21±0.033	1.42±0.02	0.043±0.01
DF11	4.55±0.037	1.61±0.009	1.0±0.03	0.048±0.02
JM109	6.64±0.138	1.05±0.025	1.69±0.01	0.21±0.05

[a]Standard deviation from duplicate experiments

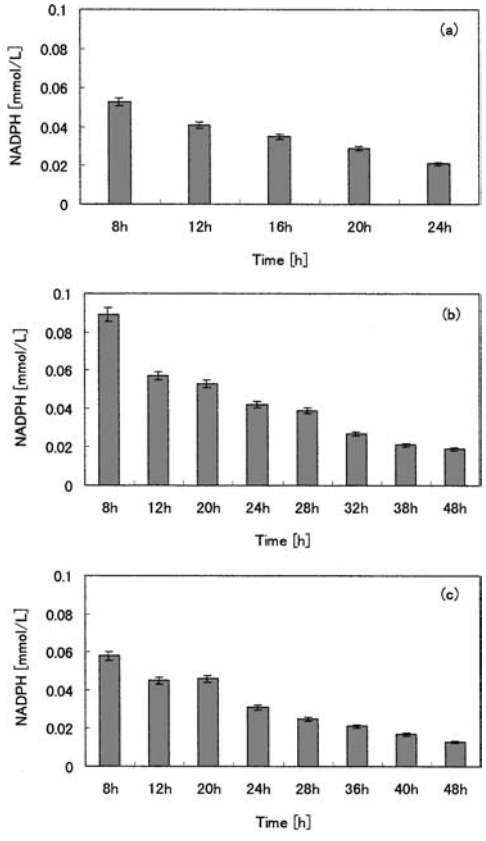

Fig. 3 NADPH concentration in **a** *E. coli* JM109, **b** *E. coli* DF11, and **c** *E. coli* DF11/pAeKG1. *Error bars* Standard deviation from three measurements

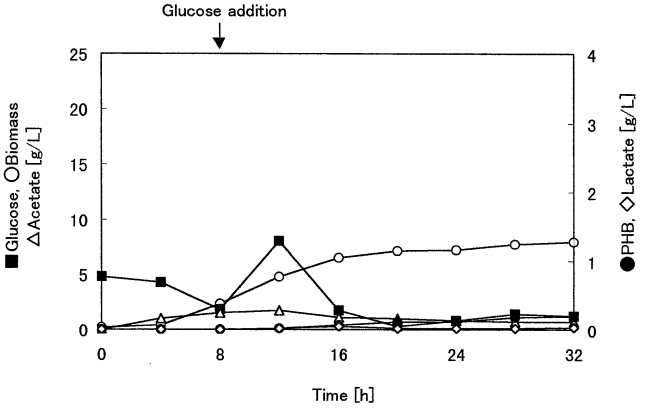

Fig. 4 Results of fed-batch fermentation of *E. coli* DF11/pAeKG1; the initial glucose concentration was 5 g/l

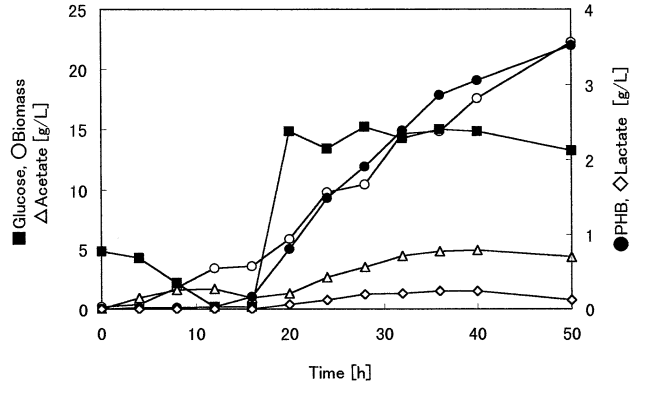

Fig. 5 Results of fed-batch fermentation of *E. coli* DF11/pAeKG1; the initial glucose concentration was 5 g/l and the glucose concentration was controlled at 15 g/l after 16 h of cultivation

growth of *pgi*-knockout *E. coli* DF11 was repressed compared with that of *E. coli* JM109. This might have been due to the overproduction of NADPH in *E. coli* DF11 in the PP pathway. When an NADPH-consuming pathway, such as the PHB synthetic pathway, was introduced, growth recovered to some extent, as shown in Fig. 2c. The intracellular NADPH was measured and compared to verify this, as shown in Fig. 3. It should be noted that the NADPH concentration decreases as the glucose concentration decreases.

Figure 4 shows the results of the fed-batch culture of *E. coli* DF11/pAeKG1, in which the initial glucose concentration was lowered to 5 g/l. As can be seen from Fig. 4, growth recovered well (highest biomass in 32 h was 7.9 g/l), while PHB production was low (compare with Fig. 2c). This might be due to the shortage of acetyl-CoA available for the PHB synthetic pathway because of the lower glucose-uptake rate. Figure 5 shows another fed-batch experimental result in which the initial glucose concentration was also 5 g/l as before but the glucose concentration was increased and maintained at 15 g/l after 16 h of cultivation to supply acetyl-CoA using the glucose sensor with feedback control. As expected, growth was enhanced (maximum cell concentration of about 23 g/l at 50 h) and final PHB concentration also increased (up to 3.53 g/l).

It is quite important to understand how heterologous polymer accumulation affects cell metabolism. We previously compared the global protein expression patterns with respect to culture conditions using 2D gel electrophoresis (Kabir and Shimizu, 2001). Here, we investigat-

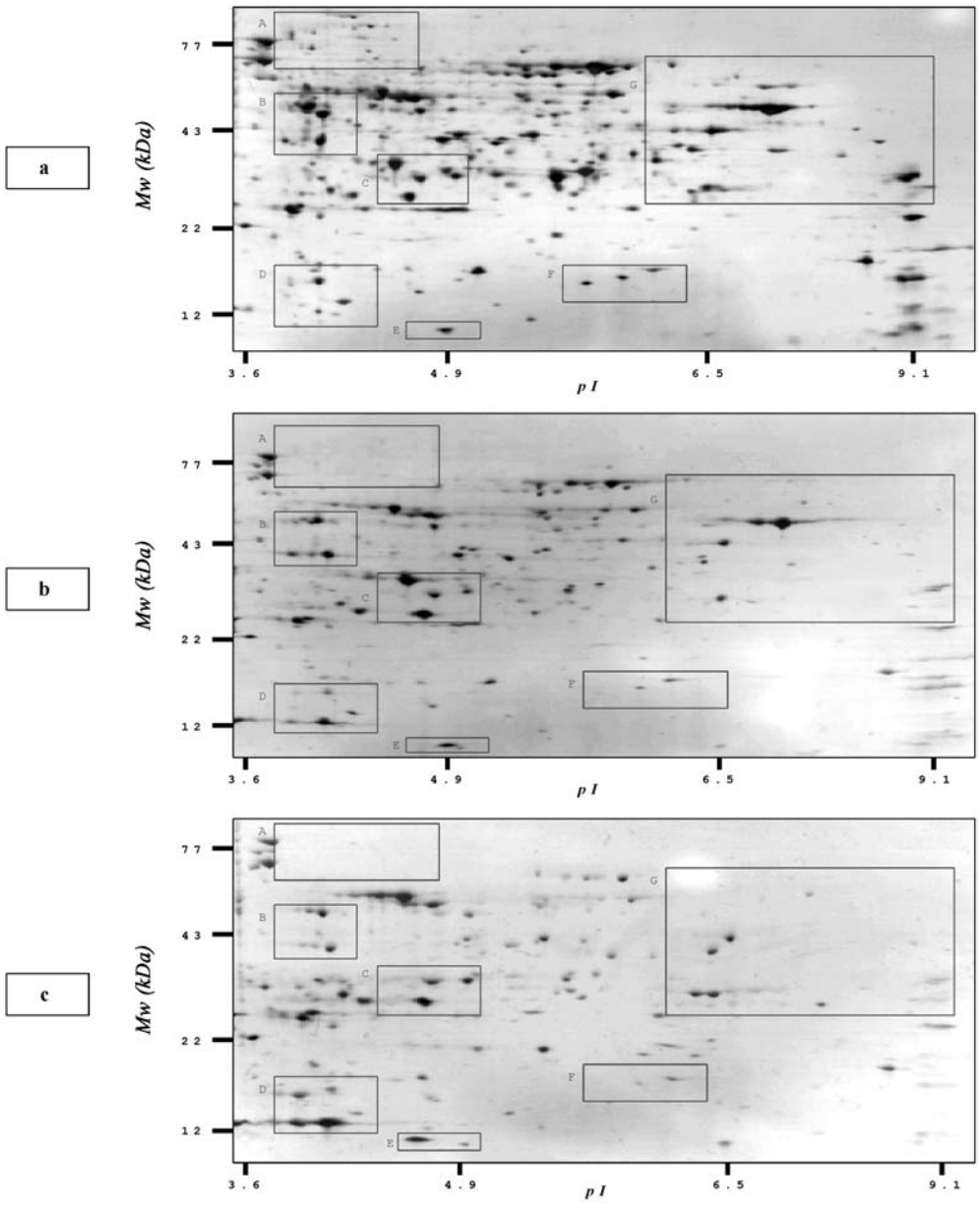

Fig. 6 Silver-stained proteome map of intracellular proteins expressed in *pgi*-knockout *E. coli* DF11/pAeKG1 (**a**), *E. coli* DF11 (**b**) and *E. coli* JM109 (**c**). The seven areas with differentially expressed protein spots are marked *A–G*

ed differential pattern of protein expression in the different strains. The gene expression profiles at the protein level of *E. coli* DF11/pAeKG1, *E. coli* DF11 and *E. coli* JM109 at the time indicated by the arrow in Fig. 2 are shown in Fig. 6. To compare the relative expression level of cellular proteins, equivalent amounts of protein from each sample were loaded on 2D gels. The overall profiles of the synthesized proteins within pI ranges between 3 and 10 were quite reproducible and distinctive enough to be compared and matched even by the naked eye.

Silver-stained gels were scanned, and 22 differentially expressed proteins (Fig. 7, spots 1–8 within region A; spot 3 within region B; spots 4 and 5 within region C; spot 4 within region D; spot 1 within region E; spot 1 within region F and spots 1, 5–11 within region G) were selected for further identification by MALDI-TOF mass spectrometry. Of the 22 protein spots, 12 could be identified by a database search based on the peptide-mass fingerprinting method for the respective spot according to the method of Henzel et al. (1993). The characterization and identification of differentially expressed proteins excised from the 2D gels of *E. coli* DF11/pAeKG1, *E. coli* DF11 and *E. coli* JM109 are summarized in Table 2. As a specific example, spot 4 within region C in Fig. 7 (designated as spot C4 in Table 2) was unambiguously identified as malonyl CoA-acyl carrier protein transacylase, encoded by *fabD* of *E. coli* (SWISS-2DPAGE accession no. P25715) by database searching. As shown in Table 3, the PeptIdent search gave a positive match with a sequence with more than 33% similarity (135 amino acids out of 309) which far exceeded the score of

Table 2 Identification and characterization of differentially expressed proteins from silver-stained 2D electrophoretic gels of *Escherichia coli* DF11/pAeKG1, DF11 and JM109 as shown in Fig. 7. *MM* Molecular mass in kilodaltons

Spot[a]	pI/ MM	SWISS-2D-PAGE accession no.	Gene (encoded protein)	Peptide sequences utilized in identification
A1	–	–	–	–
A2	–	–	–	–
A3	–	–	–	–
A4	4.6/67.2	P02349	*rpsA* (30S ribosomal protein S1)	ASEASRDR ERISLGVK DTLHLEGK NRAISLSVR ERTRVSLGLK LDQKRNNVVVSR GATVELADGVEGYLR VKHPSEIVNVGDEIT VK DRVEDATLVLSVGDE
A5	–	–	–	–
A6	–	–	–	–
A7	–	–	–	–
A8	–	–	–	–
B3	4.4/44.2	P39172	*znuA* (high-affinity zinc-uptake system protein)	LVELMPQSR MGTLDPLGTNIK GYFVFHDAYGYFEK LVELMPQSRAKLDAN LK ATAVAIHGKLVELMP QSRAK TSYSEFLSQLANQYA SCLK LPGAKQVTIAQLEDV KPLLMK
C4	4.9/33.4	P25715	*fabD* (malonyl CoA-acyl carrier protein transacylase)	VLTGLTKR VWQQQGGK EAVERAGAACK QLYNPVQWTK ITFNAPTVPVVNNVD VK DALVRQLYNPVQWTK ALPLPVSVPSHCALM KPAADK RALPLPVSVPSHCAL MKPAADK RIVDTLTASALNEPS AMAAALEL
C5	4.8/35.8	P23861	*potD* (spermidine/putrescine-binding periplasmic protein)	GSLLLTDDAR EVFQMALRK KLGYSGNTTDPK QVAETIGYPTPNLAAR EGGIFWMDSLAIPANAK GSLLLTDDAREVFQMALR
D4	4.3/16.0	P21346	*greA* (transcription elongation factor greA)	EQQGFCEGR LREELDFLK EQQGFCEGRIK GAEKLREELDFLK EQQGFCEGRIKDIEAK
E1	4.8/11.3	P26605	*hdeB* (protein hdeB)	KNPQKNLYTFK NLYTFKNQASNDLPN AMTPVAWWMLHEETVYK ANESAKDMTCQEFID LNPK NPQKNLYTFKNQASN DLPN
F1	5.6/15.5	P29209	*ibpA* (16-kDa heat-shock protein A)	TYLYQGIAER ERTYLYQGIAER TYLYQGIAERNFERK MRNFDLSPLYRSAIG FDR GAHADEQKERTYLYQ GIAER
G1	6.3/36.7	P06977	*gapA* (glyceraldehyde 3-phosphate dehydrogenase A)	KHITAGAKK VLDLIAHISK VTAERDPANLK IGRIVFRAAQK TVDGPSHKDWR VPTPNVSVVDLTVR YDSTHGRFDGTVEVK AATYEQIKAAVKAAA EGEMK DWRGGRGASQNIIPS STGAAK LTGMAFRVPTPNVSV VDLTVR

Table 2 (continued)

Spot[a]	pI/MM	SWISS-2D-PAGE accession no.	Gene (encoded protein)	Peptide sequences utilized in identification
G5	7.3/25.2	P10344	*glnH* (glutamine-binding periplasmic protein)	ANNNDVKSVK ENGTYNEIYK ENGTYNEIYKK SGTGSVDYAKANIKTK VVAVKSGTGSVDYAKANIK AIDFSDGYYKSGLLVMVK ENGTYNEIYKKWFGTEPK
G6	7.1/37.3	P45523	*fkpA* (FKBP-type peptidyl-prolyl *cis-trans* isomerase)	EKFAKEK FAKEKGVK GKEYREK SSAQAKMEK EFDNSYTR AAFKNDDQK LVIPPELAYGK MEKDAADNEAK GEAPKDSDTVVVNYK GVKTSSTGLVYQVVE AGK
G7	–	–	–	–
G8	7.4/36.0	P37903	*ynaF* (unknown protein)	SQLEEIIK DRILELAKK AEAKSQLEEIIKK LPTDRVHVHVEEGSPK TILVPIDISDSELTQR FKLPTDRVHVHVEEGSPK MNRTILVPIDISDSELTQR
G9	–	–	–	–
G10	–	–	–	–
G11	8.8/42.6	P05053	*ptsG* (glucose phophotransferase enzyme IIBC[Glc])	ALDLKTPGR TEMDEYIR TPGREDATEDAK LPEYLGFFAGKR VSVADVSKVDQAGLK IKLPEYLGFFAGKR FYRIKLPEYLGFFAGK HLADTGVLGGIISGA IAAYMFNR

[a] A, B, C, D, E, F, and G represent the particular regions as shown in Fig. 7

Table 3 An example of characterization of the spot C4 (as shown in Table 2) by database search using the PeptIdent server. *MM* Molecular mass in kilodaltons

Score	Sequence covered	SWISS-2DPAGE accession no.	Protein description	pI/MM
0.69	33.4%	P25715	Malonyl CoA-acyl carrier protein transacylase (EC 2.3.1.39) (MCT); *Escherichia coli*	4.95/32,286.01
0.38	2.4%	Q8VQR2	Efa1; *E. coli*	6.49/36,5795.64
0.38	2.4%	Q9RM48	Lymphostatin; *E. coli*	6.44/36,5969.00
0.38	2.4%	Q9RPH1	EHEC factor for adherence; *E. coli*	6.44/36,5954.99
0.38	10.9%	Q47281	Type I restriction enzyme *Eco*EI R protein (EC 3.1.21.3) (R.EcoEI); *E. coli*	5.28/92,627.02

the subsequent four entries. The theoretical isoelectric point (pI) and molecular mass (MM) were also compared with the observed pI and MM of the spot visualized on the gel (Fig. 6a). When the 2D gel electrophoresis results of *E. coli* DF11/pAeKG1 and *E. coli* DF11 were compared with those of *E. coli* JM109, the proteins encoded by *greA, hdeB, glnH* and *ptsG* were found to be present in the latter strain but not in the former two strains. When the 2D gel electrophoresis results from *E. coli* DF11/pAeKG1 were compared with those from *E. coli* DF11 and *E. coli* JM109, it was observed that the presence of plasmid pAeKG1 significantly altered protein expression, as evidenced in Fig. 6a by the expression of more genes encoding proteins visualized on 2D gel electrophoresis. Variations in the accumulation of PHB in *E. coli* DF11/pAeKG1 were the result of expression of proteins encoded by *rpsA, znuA, fabD, potD, fkpA, gapA, ynaF* and *ibpA*. The expression of *potD*- and *fkpA*-encoded proteins was observed in both the recombinant *pgi* mutant carrying *phb* and the *pgi* mutant lacking *phb* ; however,

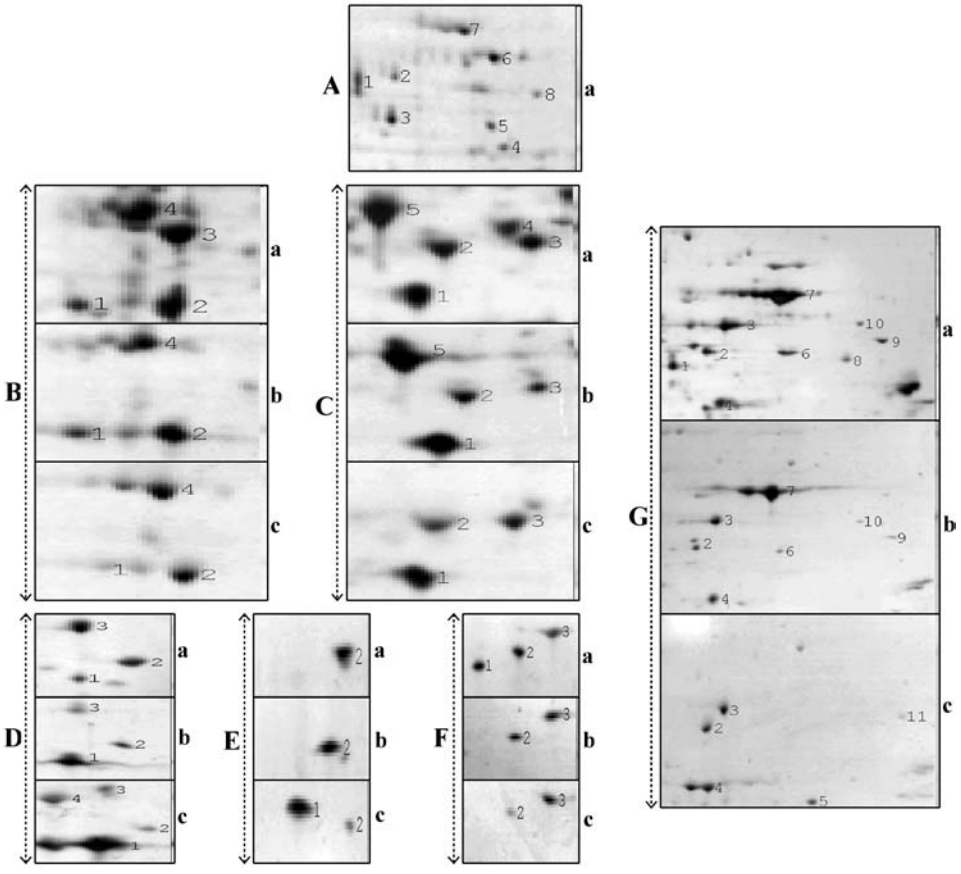

Fig. 7 Enlarged view of regions *A–G* from Fig. 6a, b, and c. *Numbers* on the right side of each spot within the gel images correspond to the individual proteins; *a*, *b* and *c* on the right side of each frame represent the enlarged part of the respective regions indicated in Fig. 6a, b, and c, respectively

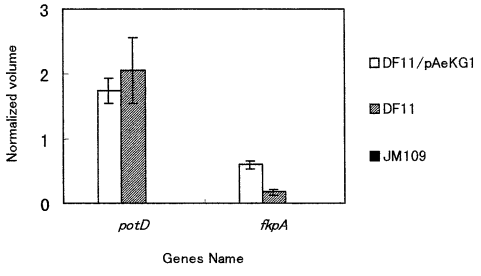

Fig. 8 Quantification of identified protein spots showing altered expression level. Spot intensities were measured and normalized as described in Materials and methods. Proteins encoded by potD and fkpA were not detected on 2D gel electrophoresis of E.coli JM109, perhaps due to lower expression of the respective mRNAs. *Error bars* Standard deviations from duplicate gels

the amounts of synthesized proteins as determined by the software Image Master 2D Elite varied (Fig. 8). Up-regulation of the protein expressed by *fkpA* (FKBP-type peptidyl-prolyl *cis-trans* isomerase) in *E. coli* DF11/pAeKG1 might reduce the stress response caused by the presence of the plasmid, since the *fkpA*-encoded protein plays an active role either as a folding catalyst or as a chaperone in extracytoplasmic components (Missiakas et al. 1996).

Discussion

The inactivation of *pgi* forces glucose metabolism to proceed via the PP pathway. Metabolic flux ration (METAFoR) analysis by NMR has shown that a minor fraction of glucose catabolism occurs via the Entner-Doudoroff pathway in both *E. coli* wild-type and the *pgi* mutant strain (Canonaco et al. 2001). Examination of the operational catabolic pathways and their flux ratios using [U-^{13}C6]-glucose-labeling experiments and metabolic flux ratio analysis provided evidence for PP pathway as the primary route of glucose catabolism in the *pgi* mutant (Canonaco et al. 2001). The resulting extensive flux through the PP pathways apparently disturbs the reducing-power balance in the *pgi* mutant perhaps due to the difficulty in reoxidizing NADPH and the inability of the PP pathway to support higher fluxes.

To verify that insufficient reoxidation of NADPH is relevant in disturbing the reducing-power balance in the *pgi* mutant, a 9.8-kb plasmid, pAeKG1, containing the *phbCAB* operon and *parB* locus was transformed in the *pgi* mutant *E. coli* since the enzyme acetoacetyl-CoA reductase is NADPH-mediated. Basically, reoxidation of NADPH can potentially be achieved by three reactions in *E. coli*: (1) by the NADPH-dependent malic enzyme; (2) by the membrane-bound transhydrogenase *pntAB* (Clarke et al. 1986); and (3) by the soluble transhydrogenase *udhA* (Boonstra et al. 1999) (Fig. 1). Significant involvement of

malic enzyme in NADPH reoxidation can be excluded because virtually no pyruvate originates from malate (Canonako et al, 2001), and this result was consistent with our finding of no malic enzyme activity. Similarly, *pntAB* is unlikely to catalyze sufficient reoxidation of NADPH since *pgi pntAB* double mutants grew as slowly as the *pgi* mutant (Hanson and Rose 1980), which means that additional knockout of *pntAB* does not further reduce the rate of glucose catabolism. The primary metabolic function of *pntAB* appears to be in the generation of NADPH, since *zwf pnt* double mutants grew slower than the *zwf* mutant (Hanson and Rose 1980), as would be expected when *pntAB* produces NADPH in the absence of glucose metabolism via the PP pathway. Overexpression of soluble transhydrogenase *udhA* in the *pgi* mutant *E. coli* increased the specific growth rate by about 25%, providing evidence of the activity of soluble transhydrogenase *udhA* in the reoxidation of NADPH (Canonako et al, 2001). In our study, it was observed that expression of *phb* in the *pgi* knockout *E. coli* resulted in increased biomass production (Fig. 2c) compared with the *pgi* mutant lacking *phb* (Fig. 2b). Obviously, PHB accumulation within cells increases the overall biomass concentration even though the growth rate becomes slower. Thus, calculation of true cell mass by subtracting the PHB concentration from the biomass is recommended to determine the actual biomass compared with that of non-PHB producers. Expression of *phb* in *E. coli* DF11/pAeKG1 increased the true cell mass by about 19%, suggesting a possible physiological role for acetoacetyl-CoA reductase encoded by *phbB* in the reoxidation of NADPH. The measurement of NADPH concentration supported our experimental observations, since the concentration of NADPH was much higher in *E. coli* DF11 than that of *E. coli* DF11/pAeKG1 and JM109.

We also studied the effect of different carbon sources to understand the fermentation characteristics of *pgi* mutants. Under aerobic condition, the mutants grew well on fructose as the sole carbon source, as was reported previously (Fraenkel and Levisohn 1967). This indicates that glucose-6-phosphate is not an essential metabolite for *E. coli* biomass synthesis since it cannot be formed from fructose in the *pgi* mutant. However, the final PHB concentration was about 1.0 g/l (data not shown). Gluconate was also used and a similar PHB concentration was obtained (data not shown). The decreased amount of PHB production in cells grown on fructose or gluconate as carbon source was due to the shortage of NADPH. A fair amount of acetate was produced in the presence of these carbon sources. In another experiment, in which glycerol served as carbon source, cell growth was relatively high and acetate production lower, but PHB production was less than 1 g/l (data not shown) due to less NADPH production.

Proteome analysis demonstrated that *ptsG*, which codes for a transport protein for glucose uptake that is a component of the PTS transport system, was not expressed in either of the *pgi* mutants (*E. coli* DF11/pAeKG1 and *E. coli* DF11). Recently, Kimata et al. (2001) proposed that *pgi* mutation leads to a block in the glycolytic pathway, which accelerates RNaseE-mediated degradation of *ptsG* transcripts. Their observation is in good agreement with our proteome analysis results. Degradation of the *ptsG* transcript might be one of the reasons for less glucose consumption and thus low biomass concentration in *pgi* mutants.

Metabolically engineered *E. coli* strains may undergo physiological changes upon accumulation of PHB, which is not a normal metabolite of *E. coli* and which may be considered as a stress on the cells inducing the heat-shock response. Indeed, the levels of heat-shock proteins encoded by genes such as *dnaK, groEL, groES, clpB, grpE, hslV, htpG* and *ibpA* were found to be significant (Kabir and Shimizu 2001; Han et al. 2001). The increased expression of the protein encoded by *fkpA* in *E. coli* DF11/pAeKG1 (Fig. 8) is consistent with this observation, since the *fkpA* protein plays an active role either as folding catalysts or as chaperones in extracytoplasmic compartments (Missiakas et al. 1996). Furthermore, the accumulation of PHB granules in the cytosolic space would disturb the normal intracellular architecture, such as chromosomal attachment, which would also result in the heat-shock response. Bacteria naturally accumulating PHB synthesize phasin protein, which covers the surface of PHB granules. *E. coli* does not produce PHB naturally and therefore does not have the phasin gene (Wieczorek et al. 1995); consequently, the hydrophobic PHB granules are in direct contact with intracellular biomolecules including DNA, RNA, and proteins. Certainly, this acts as a major stress on the cells for several possible reasons including protein denaturation on the surface of PHB granules. This unfavorable condition generated by PHB accumulation may explain the high level of *rpsA* (encoding 30S ribosomal protein S1) expression in *E. coli* DF11/pAeKG1, and it seems to have caused a further increase in the total amount of soluble protein (Table 1). S1 is the largest ribosomal protein (Wittmann 1974); it is present in the small subunit of the *E. coli* 70S ribosome and has a pivotal role in stabilizing mRNA on the ribosome for protein synthesis (Sengupta et al. 2001). Moreover, S1 has been reported to be necessary in some cases for translation initiation (Tzareva et al. 1994) and for translation elongation (Potapov and Subramanian 1992). In a study by Arnold et al. (2001), *rpsA* expression was due to acetate accumulation. However, in our study, the high-level expression of *rpsA* in *E. coli* DF11/pAeKG1 could not have been due to acetate accumulation since acetate would have been expected to cause decreased expression . Instead, the high amounts of soluble protein synthesis in the *pgi* mutant carrying *phb* was due to the effect of PHB accumulation and ultimately resulted in *rpsA* being highly expressed. This result implies that protein synthesis in *E. coli* DF11/pAeKG1 was much increased in the presence of plasmid (Table 1).

Glyceraldehyde-3-phosphate dehydrogenase, encoded by *gapA*, is a glycolytic enzyme that catalyzes the interconversion of glyceraldehyde-3-phosphate to glycerate-1,3-diphosphate. The enzyme was detected by two-

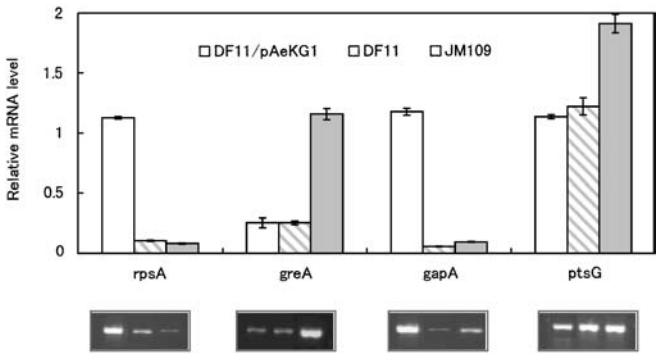

Fig. 9 Transcript levels of *rpsA, greA, gapA* and *ptsG*. *Error bars* Standard deviation from three measurements of each gene

dimensional gel electrophoresis of recombinant *pgi* mutant carrying *phb* genes (spot G1 in Fig. 7). Conversion of three of the pentose-5-phosphates into two molecules of hexose (fructose-6-phosphate) and one of triose (glyceraldehyde-3-P) occurs in a series of reactions (see Fig. 1) and the direction of the pathway varies in response to different metabolic conditions. Since glucose is metabolized exclusively via the PP pathway in the *pgi* mutant, the source of glyceraldehyde-3-P is directly from the PP pathway. Glyceraldehyde-3-P is one of the important precursor metabolites for the synthesis of isopentenyl diphosphate (IPP), which acts as a carrier in the synthesis of cell envelope and extracellular polymers (e.g. peptidoglycan, lipopolysaccharide, techoic acids). As a result, a large fraction of glyceraldehyde-3-P is consumed to maintain the glycolytic flux for biomass production and to provide precursor metabolites. Therefore, glyceraldehyde-3-phosphate dehydrogenase expression in *E. coli* DF11/pAeKG1 was highly up-regulated to enhance the rate of conversion of glyceraldehyde-3-P (first three carbon metabolite of glycolysis) to glycerate-1,3-diphosphate to meet the increasing demand for acetyl-CoA, since the PHB synthesis pathway competes for acetyl-CoA with three other metabolic pathways (Lee and Chang 1995; Lee et al. 1994b).

Expression of the protein encoded by *fabD* (malonyl CoA-acyl carrier protein transacylase, involved in the fatty-acid biosynthesis pathway) found in PHB-synthesizing *E. coli* DF11/pAeKG1 cells indicates that a large fraction of acetyl-CoA was channeled to fatty-acid synthesis, as evidenced by the low yield of PHB. Although the biological function of the*ynaF*-encoded protein is not clear yet, this protein has been reported to be expressed in plasmid-containing cells (Link et al. 1997). This is most likely the reason why *ynaF* was expressed only in PHB-accumulating cells. *E. coli* JM109 consumed glucose fully at 20 h (Fig. 2a); thereafter, cells were forced to consume organic acid, which accumulated in the culture broth after 20 h. Organic-acid consumption was activated the glyoxylate shunt, which ultimately limited glutamine synthesis. This probably explains why *glnH* was highly expressed in *E. coli* JM109. The protein encoded by *potD* is necessary for maximal spermidine and putrecine transport activity and was up-regulated in *E. coli* DF11 cells (Fig. 8). Although the biological function of the *potD* protein remains unclear, it might have an effect on nucleic acid structure and on protein synthesis.

High-level expression of the *hdeB* protein in *E. coli* JM109 was mainly due to the effect of acetate accumulation, consistent with the results of Arnold et al. (2001). *HdeB* is a structural homologue and forms heterodimers with the *hdeA* protein, which is required for stationary-phase acid resistance in *E. coli*. Up-regulation of the *greA*-encoded protein (transcription elongation factor) in *E. coli* JM109 might have been due to a temporary shortage of the complementary nucleotide, resulting from complete consumption of glucose at 20 h (Fig. 2a). Such temporary shortages can lead to pausing of RNA polymerase. When this occurs, restarting synthesis requires the *greA* protein to release the pause (Stebbins et al. 1995). As a result, the 3' end of the mRNA is cleaved so that it properly re-aligns within the catalytic site of the polymerase. Expression of the high-affinity zinc-uptake system protein, encoded by *znuA*, was highly up-regulated in *E. coli* DF11/pAeKG1 but the reason is unclear.

Using proteomics tools, we have identified several differentially expressed proteins. In order to verify the proteomics results, semi-quantitative RT-PCR analyses of some genes were carried out; the results are shown in Fig. 9. Since the cell's physiological state is ultimately dictated at the protein level, mRNA expression results should be complemented by proteomics data. The disappearance of proteins encoded by *rpsA, greA* and *gapA* but not *ptsG* as determined by 2D gel electrophoresis was due to the lower level of expression of the corresponding genes that was observed by RT-PCR (Fig. 9). The abundance of the *ptsG* transcript increased in *E. coli* JM109 while it was moderately reduced in the *pgi* mutants. Thus, it is apparent that *ptsG* is transcribed normally in *pgi* cells. These results strongly suggest that mutation of *pgi* affect *ptsG* expression by some unknown mechanism(s) after transcription initiation because the protein encoded by *ptsG* was not detected by 2D gel electrophoresis of *pgi* knockout *E. coli*. Kimata et al. (2001) reported that *pgi* mutation leads to a block in the glycolytic pathway, which accelerates RNaseE-mediated degradation of the *ptsG* gene transcript. This was the most probable reason why the protein encoded by *ptsG* was not detected on 2D gels of *pgi* mutants.

Acknowledgement This research was supported in part by a grant from New Energy and Industrial Technology Development Organization (NEDO) of the Ministry of Economy, Trade and Industry of Japan (Development of Technological Infrastructure for Industrial Bioprocess Project).

References

Arnold CN, Mcelhanon J, Lee A, Leonhart R, Siegele DA (2001) Global analysis of *Escherichia coli* gene expression during the acetate-induced acid tolerance response. J Bacteriol 183:2178–2186

Bergmeyer HU, (1989) Methods of enzymatic analysis, vol VII, 3rd edn. VCH, Weinheim, Germany

Blackstock WP, Weir MP (1999) Proteomics: quantitative and physical mapping of cellular proteins. Trends Biotechnol 17:121–127

Boonstra B, French CE, Wainwright I, Bruce NC (1999) The *udhA* gene of *Escherichia coli* encodes a soluble pyridine nucleotide transhydrogenase. J Bacteriol 181:1030–1034

Braunegg G, Sonnteither B, Lafferty RM (1978) A rapid gas chromatography method for the determination of poly-β-hydroxybutyric acid in microbial biomass. Eur J Appl Microbiol Biotechnol 6:29–37

Canonaco F, Hess TA, Heri S, Wang T, Szyperski T, Sauer U (2001) Metabolic flux response to phosphoglucose isomerase knock-out in *Escherichia coli* and impact of overexpression of the soluble transhydrogenase UdhA. FEMS Microbiol Lett 204:247–252

Clarke DM, Loo TW, Gillam S, Bragg PD (1986) Nucleotide sequence of the *pntA* and *pntB* genes encoding the pyridine nucleotide transhydrogenase of *Escherichia coli*. Eur J Biochem 158:647–653

Fraenkel DG, Levisohn SR (1967) Glucose and gluconate metabolism in an *Escherichia coli* mutant lacking phosphoglucose isomerase. J Bacteriol 93:1571–1578

Han M-J, Yoon SS, Lee SY (2001) Proteome analysis of metabolically engineered *Escherichia coli* producing poly (3-hydroxybutyrate). J Bacteriol 183:301–308

Hanson RL, Rose C (1980) Effects of insertion mutation in a locus affecting pyridine nucleotide transhydrogenase (*pnt*::Tn5) on the growth of *Escherichia coli*. J Bacteriol 141:401–404

Henzel WJ, Billeci TM, Stults JT, Wong SC, Grimley C, Watanabe C (1993) Identifying proteins from two-dimensional gels by molecular mass searching of peptide fragments in protein databases. Proc Natl Acad Sci USA 90:5011–5015

Hochstrasser DE (1998) Proteome in perspective. Clin Chem Lab Med 36:825–836

Hochstrasser DF, Harrington MG, Hochstrasser AC, Miller MJ, Merril CR (1988) Methods for increasing the resolution of two-dimensional protein electrophoresis. Anal Biochem 173:424–435

Kabir MM, Shimizu K (2001) Proteome analysis of a temperature-inducible recombinant *Escherichia coli* for poly-β-hydroxybutyrate production. J Biosci Bioeng 92:277–284

Kalousek S, Lubitz W (1995) High-level poly(β-hydroxybutyrate) production in recombinant *Escherichia coli* in sugar free complex medium. Can J Microbiol 41:216–221

Kidwell J, Valentin HE, Dennis D (1995) Regulated expression of the *Alcaligenes eutrophus pha* biosynthesis gene in *Escherichia coli*. Appl Environ Microbiol 61:1391–1398

Kimata K, Tanaka Y, Inada T, Aiba H (2001) Expression of the glucose transporter gene, *ptsG*, is regulated at the mRNA degradation step in response to glycolytic flux in *Escherichia coli*. EMBO J 20:3587–3595

Lee SY (1994) Suppression of filamentation in recombinant *Escherichia coli* by amplified *ftsZ* activity. Biotechnol Lett 16:1247–1252

Lee SY, Chang HN (1995) Production of poly(3-hydroxybutyric acid) by recombinant *Escherichia coli* strains: genetic and fermentation studies. Can J Microbiol 41:207-215

Lee SY, Yim KS, Chang HN (1994a) Construction of plasmids, estimation of plasmid stability, and use of stable plasmids for the production of poly(3-hydroxybutyric acid) in *Escherichia coli*. J Biotechnol 32:203–211

Lee SY, Lee KM, Chang HN, Steinbüchel A (1994b) Comparison of recombinant *Escherichia coli* strains for synthesis and accumulation of poly(3-hydroxybutyric acid) and morphological changes. Biotechnol Bioeng 44:1337–1347

Link AJ, Robison K, Church GM (1997) Comparing the predicted and observed properties of proteins encoded in the genome of *Escherichia coli* K-12. Electrophoresis 18:1259–313

Lowery OH, Rosbrough JN, Farr AL, Randall RJ (1951) Protein measurement with the folin-phenol regent. J Biol Chem 193:265–275

Missiakas D, Betton J-M, Raina S (1996) New components of protein folding in extracytoplasmic compartments of *Escherichia coli* SurA, FkpA and Skp/OmpH. Mol Microbiol 21:871-884

O'Farrell PH (1975) High resolution two-dimensional electrophoresis of proteins. J Biol Chem 250:4007–4021

Pappin DJ, Hojrup P, Bleasby A (1993) Rapid identification of proteins by peptide-mass fingerprinting. Curr Biol 3:327–332

Patterson SD (2000) Mass spectrometry and proteomics. Physiol Genomics 2:59–65

Peoples OP, Sinskey AJ (1989) Poly-β-hydroxybutyrate biosynthesis in *Alcaligenes eutrophus* H16. Identification and characterization of the PHB polymerase gene (*phbC*). J Biol Chem 264:15298–15303

Persidis A (1998) Proteomics. Nat Biotechnol 16:393–394

Potapov AP, Subramanian AR (1992). Biochem Int 27:745–753

Rosenfeld J, Capdevielle J, Guillemot J, Ferrara P (1992) In-gel digestion of proteins for internal sequence analysis after one-or two dimensional gel electrophoresis. Anal Biochem 203:173–179

Salas M, Vinuela E, Sols A (1965) Spontaneous and enzymatically catalyzed anomerization of glucose-6-phosphate and anomeric specificity of related enzymes. J Biol Chem 240:561–568

Schubert P, Steinbuchel A, Schlegel HG (1988) Cloning of the *Alcaligenes eutrophus* poly-β-hydroxybutyrate synthetic pathway and synthesis of PHB in *Escherichia coli*. J Bacteriol 170:5837–5847

Sengupta J, Agrawal RK, Frank J (2001) Visualization of protein S1 within the 30S ribosomal subunit and its interaction with messenger RNA. Proc Natl Acad Sci USA 98:11991–6

Shi H, Nikawa J, Shimizu K (1999) Effect of modifying metabolic network on poly-3-hydroxybutyrate biosynthesis in recombinant *Escherichia coli*. J Biosci Bioeng 87:666–677

Shi H, Kyuwa K, Takasu M, Shimizu K (2001) Temperature-induced expression of *phb* genes in *Escherichia coli* and effect of temperature patterns on the production of poly-3-hydroxybutyrate. J Biosci Bioeng 91:21–26

Shevchenko A, Wilm M, Vorm O, Mann M (1996) Mass spectrometric sequencing of proteins from silver-stained polyacrylamide gels. Anal Chem 68:850–858

Sim SJ, Snell KD, Hogan SA, Stubbe J, Rha C, Sinskey AJ (1997) PHA synthesis activity control molecular weight and polydispersity of polyhydroxybutyrate in vivo. Nat Biotechnol 15:63–67

Slater SC, Voige WH, Dennis DE (1988) Cloning and expression in *Escherichia coli* of the *Alcaligenes eutrophus* H16 poly-β-hydroxybutyrate biosynthetic pathway. J Bacteriol 170:4431–4436

Stebbins CE, Borukhov S, Orlova M, Polyakov A, Goldfarb A, Darst SA (1995) Crystal structure of the *greA* transcript cleavage factor from *Escherichia coli*. Nature 373:636–640

Tzareva NV, Makhno VI, Boni IV (1994). FEBS Lett 337:189–194

Van der Werf MJ, Guettle MV, Jain MK, Zeikus JG (1997) Environmental and physiological factors affecting the succinate product ratio during carbohydrate fermentation by *Actinobacillus sp.* 130Z. Arch Microbiol 167:332–342

Wieczorek RA, Pries A, Steinbüchel A, Mayer F (1995) Analysis of a 24-kilodalton protein associated with the polyhydroxyalkanoic acid granules in *Alcaligens eutrophus*. J Bacteriol 177:2425–2435

Wittmann HG (1974) In: Namura M, Tissieres A, Lengyel P (eds) Ribosomes. Cold Spring Harbor Laboratory, Plainview, New York, pp 93–114